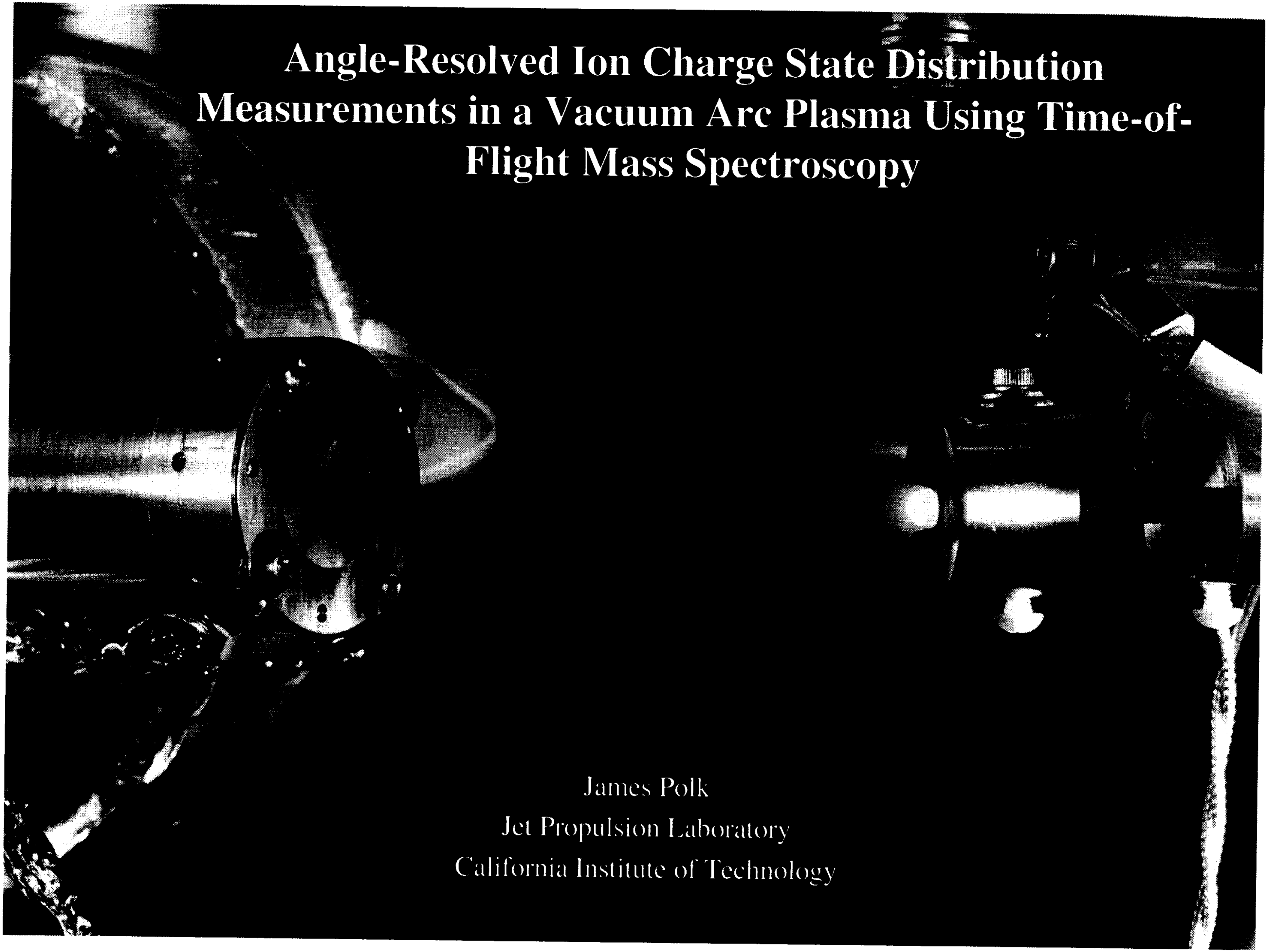

Angle-Resolved Ion Charge State Distribution Measurements in a Vacuum Arc Plasma Using Time-of-Flight Mass Spectroscopy

James Polk
Jet Propulsion Laboratory
California Institute of Technology

Cathode Spots in Vacuum Arcs Create Extreme Plasma Environments

JPL

Vacuum Arc Electron Emission Processes

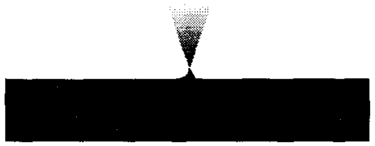

Site Initiation
Field emission from micropoint or dielectric inclusion.

Explosive Evaporation
Excessive joule heating in micro-emission site generates plasma by explosive vaporization.

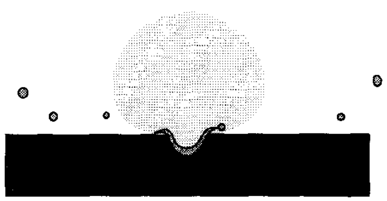

Crater Formation
Power deposited by joule heating and ion bombardment heats surface to extreme temperatures. Electrons emitted by thermal-field emission.

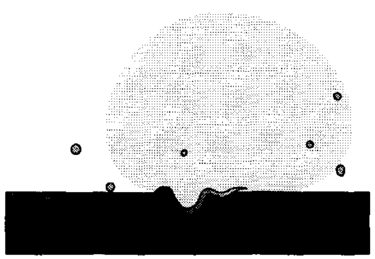

New Site Formation
Decreasing power density leads to site extinction and field emission at a nearby micropoint causes spot to shift.

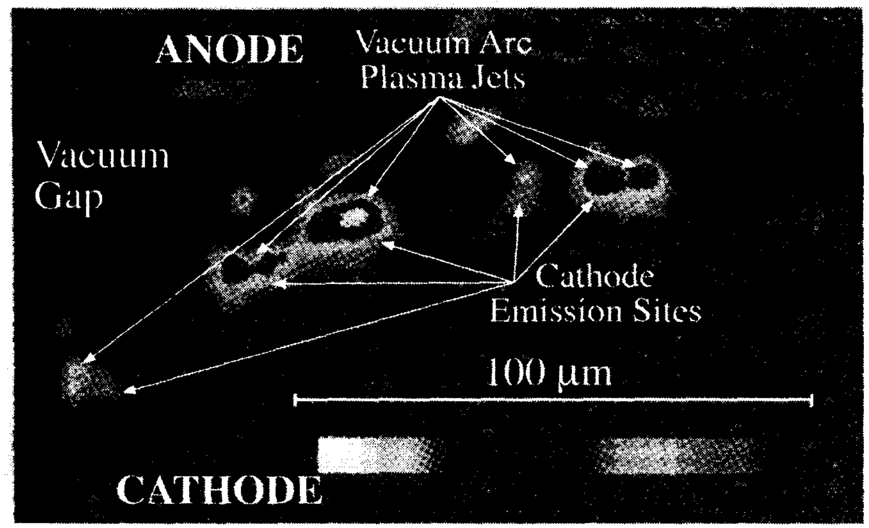

Laser absorption image shows ultra-high density plasma plumes created by cathode emission sites in a vacuum arc

- Vacuum arcs generate environments with unique properties
  - Current densities of 10^8 A/cm^2
  - Surface heat fluxes of 10^8--10^9 W/cm^2
  - Plasma densities of 10^{20}--10^{21} cm^{-3} (nearly the density of the solid metal!)
  - Nearly 100% ionization of metal vapor
  - Plasma expansion velocities of 10^4 m/s
- Pressure ionization, not electron bombardment processes, creates plasma efficiently in a tiny volume

Exploiting Extreme Conditions in Vacuum Arc Plasmas for Propulsion

JPL

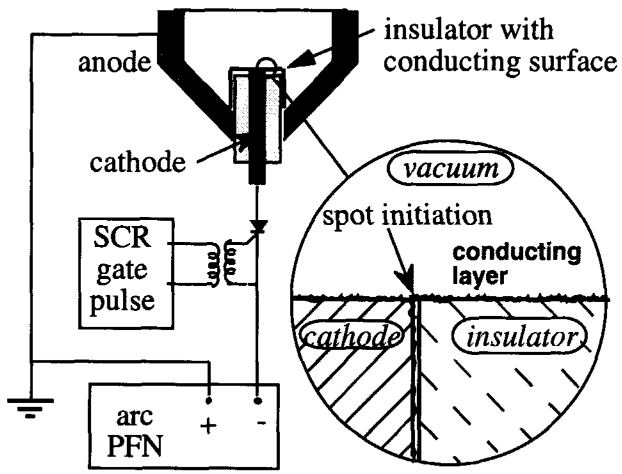

Schematic of a vacuum arc thruster

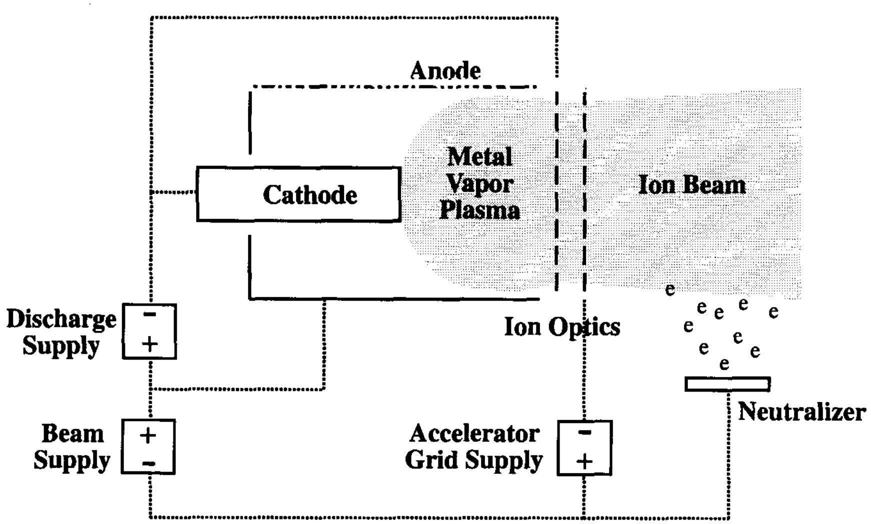

Schematic of a vacuum arc ion thruster

CONCEPT

Metal vapor plasmas can be used to produce thrust in several ways

- Direct thrust from plasma plume expansion
- Electrostatic or electromagnetic acceleration of the dense plasma

ADVANTAGES

- Vacuum arc plasma sources provide unique scaling advantages
  - No magnetic field required to confine or generate plasma
  - Plasma is created in small volume
  - No gas feed system is required
  - Discharge current can be tailored to produce wide range of plasma densities
- Plasma plume expansion allows higher current density extraction through ion optics

APPLICATIONS

- Miniaturized thrusters for microspacecraft applications
- Very high density plasmas may enable very high power thrusters

Regularities in Vacuum Arc Discharges Make Simple Performance Models Possible

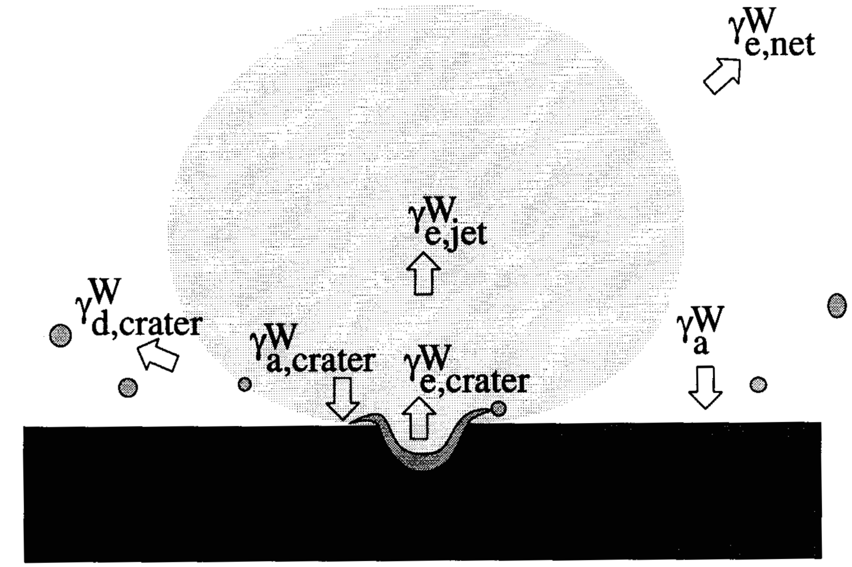

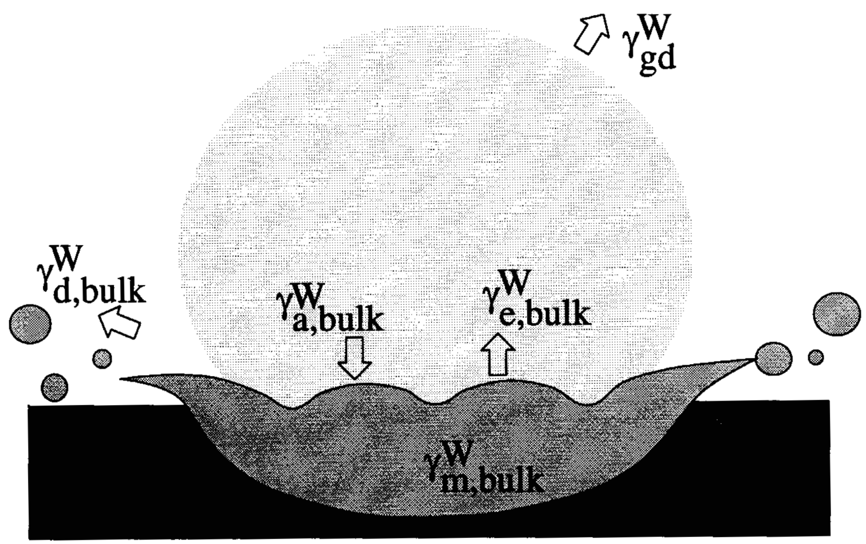

- Mass loss scales with discharge current

$$\dot{m}_t = E_r J_d,$$

- Ion current is proportional to discharge current

$$J_i = \sum_Z J_Z = f_i J_d$$

- Experiments show that fi is typically 0.07-0.1
- Ion mass loss fraction depends on f_i and E_r

$$\dot{m}_i = \sum_Z \frac{J_Z M_i}{Ze} = \frac{f_i J_d M_i}{e}\langle Z^{-1}\rangle,$$

$$\langle Z^{-1}\rangle = \sum_Z \frac{f_Z}{Z}. \qquad f_Z = \frac{J_Z}{J_i}.$$

$$F_i = \frac{f_i M_i \langle Z^{-1}\rangle}{eE_r}.$$

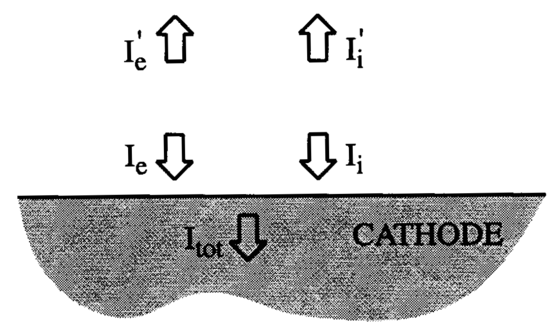

VAT Thrust is Determined by Momentum Flux Through Anode Exit

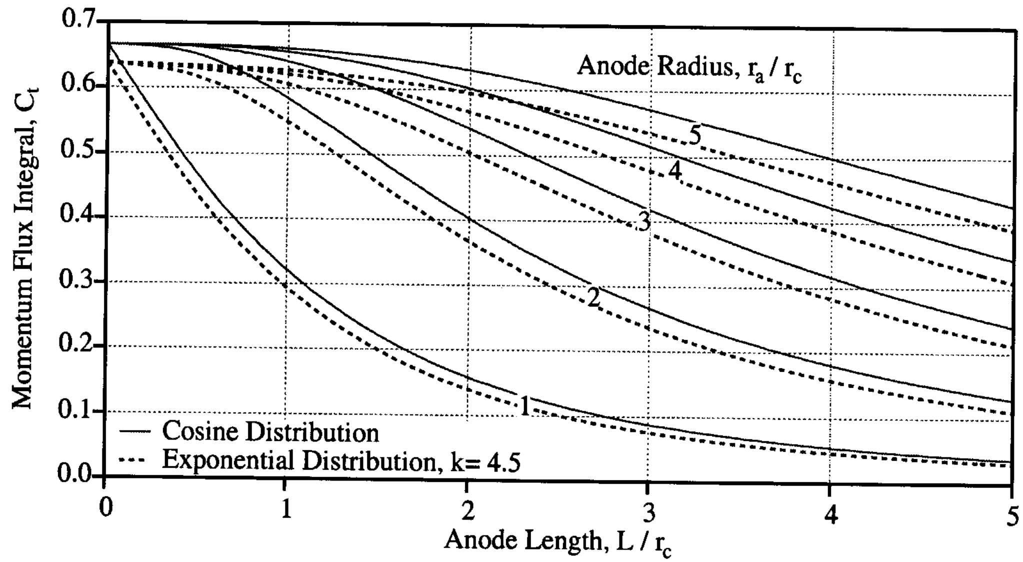

Thrust depends on material properties,operating parameters and geometry

$$dT = d\dot{m}_{ip}(l,\phi)(u_i \cos\phi)(cos\phi dA_2)$$

$$= \frac{M_i j_{ip}}{e}\langle Z^{-1}\rangle u_i \cos^2\phi dA_2$$

$$T = \frac{M_i f_i J_d u_i}{e}\langle Z^{-1}\rangle C_t(\overline{L},\overline{r}_a)$$

$$C_t = \frac{\overline{L}^3}{\pi^2}\int_0^{2\pi}\int_0^{2\pi}\int_0^{\overline{r}_a}\int_0^1 \frac{\overline{r}_1\overline{r}_2 d\overline{r}_1 d\overline{r}_2 d\theta_1 d\theta_2}{\overline{l}^5}$$

Additional performance parameters

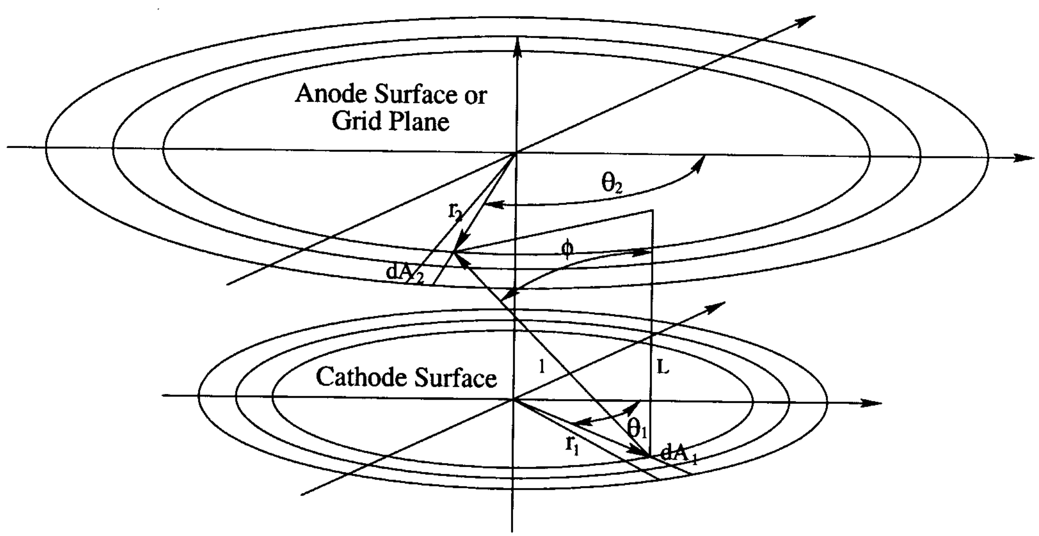

$$I_{sp} = \frac{T}{\dot{m}_t g} = \frac{M_i f_i u_i C_t}{eE_r g}\langle Z^{-1}\rangle$$

$$= \frac{F_i u_i C_t}{g}$$

$$\eta = \frac{T^2}{2\dot{m}_t P} = \frac{M_i^2 f_i^2 u_i^2 C_t^2(\langle Z^{-1}\rangle)^2}{2e^2 E_r V_d}$$

$$T/P = \frac{M_i f_i u_i C_t}{eV_d}\langle Z^{-1}\rangle$$

Angular Distribution of Ion Current

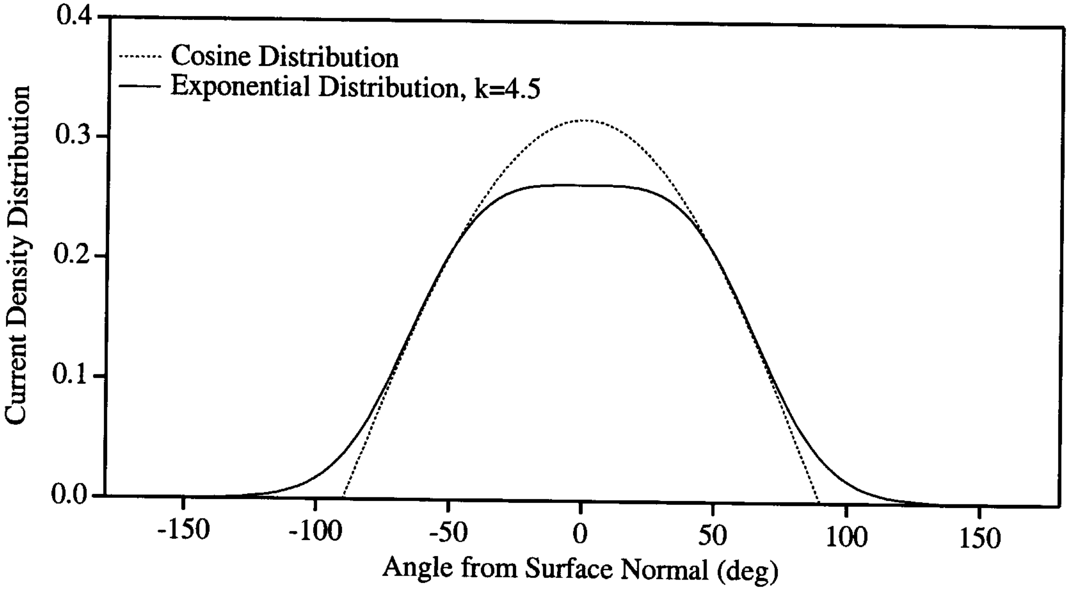

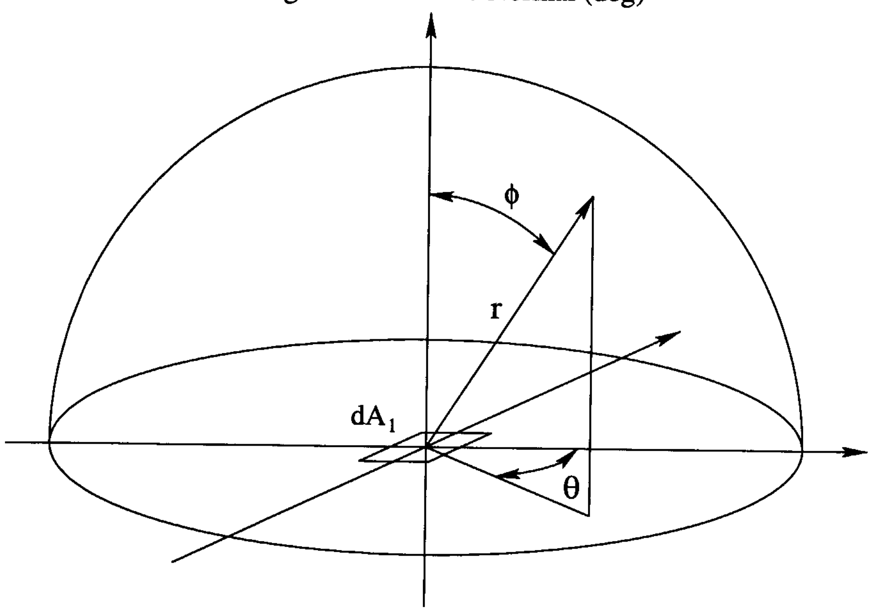

- Experiments show either a cosine or exponential distribution of ion current

$$j_{ip}(l,\phi) = \frac{j_{ic}\cos\phi dA_1}{\pi l^2}$$

$$j_{ip}(l,\phi) = \frac{2j_{ic}dA_1}{\sqrt{\pi}l^2k\,\mathrm{erf}(2\pi/k)} \times \exp(-[2\pi(1-\cos\phi)]^2/k^2)$$

Angular Distribution of Ion Energy

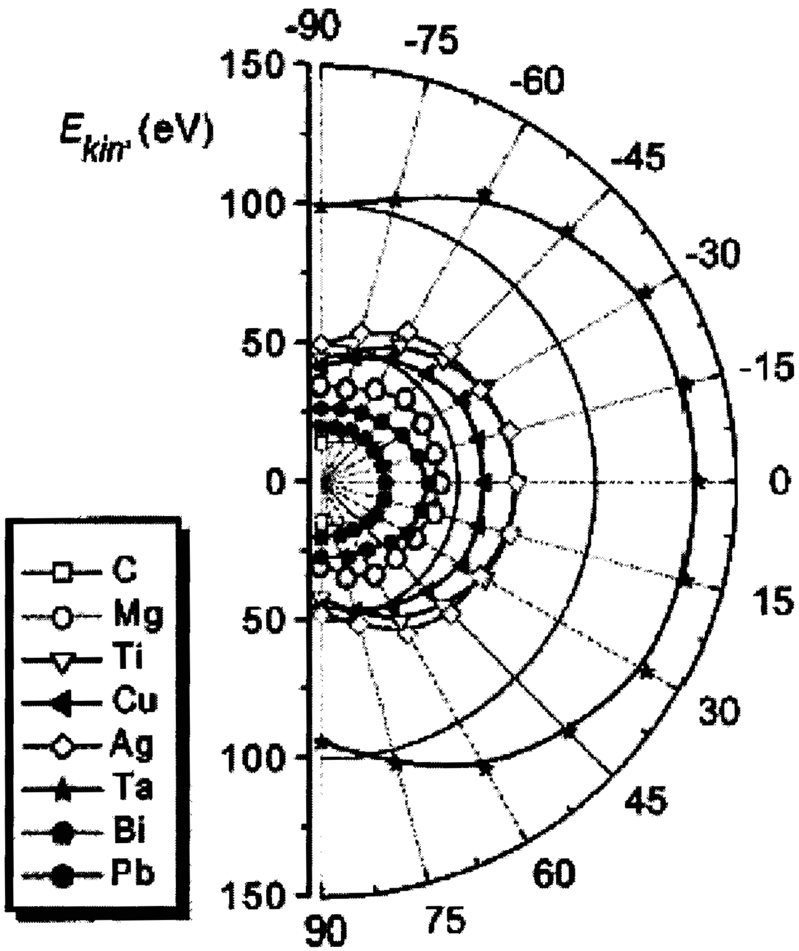

Ion energy is not a strong function of angle, as assumed in the model

Anders, A., and Yushkov, G., "Angularly resolved measurements of ion energy of vacuum arc plasmas," Appl. Phys. Lett., 80(14), pp. 2457-2459, April 8, 2002.

Time-of-Flight Mass Spectrometer

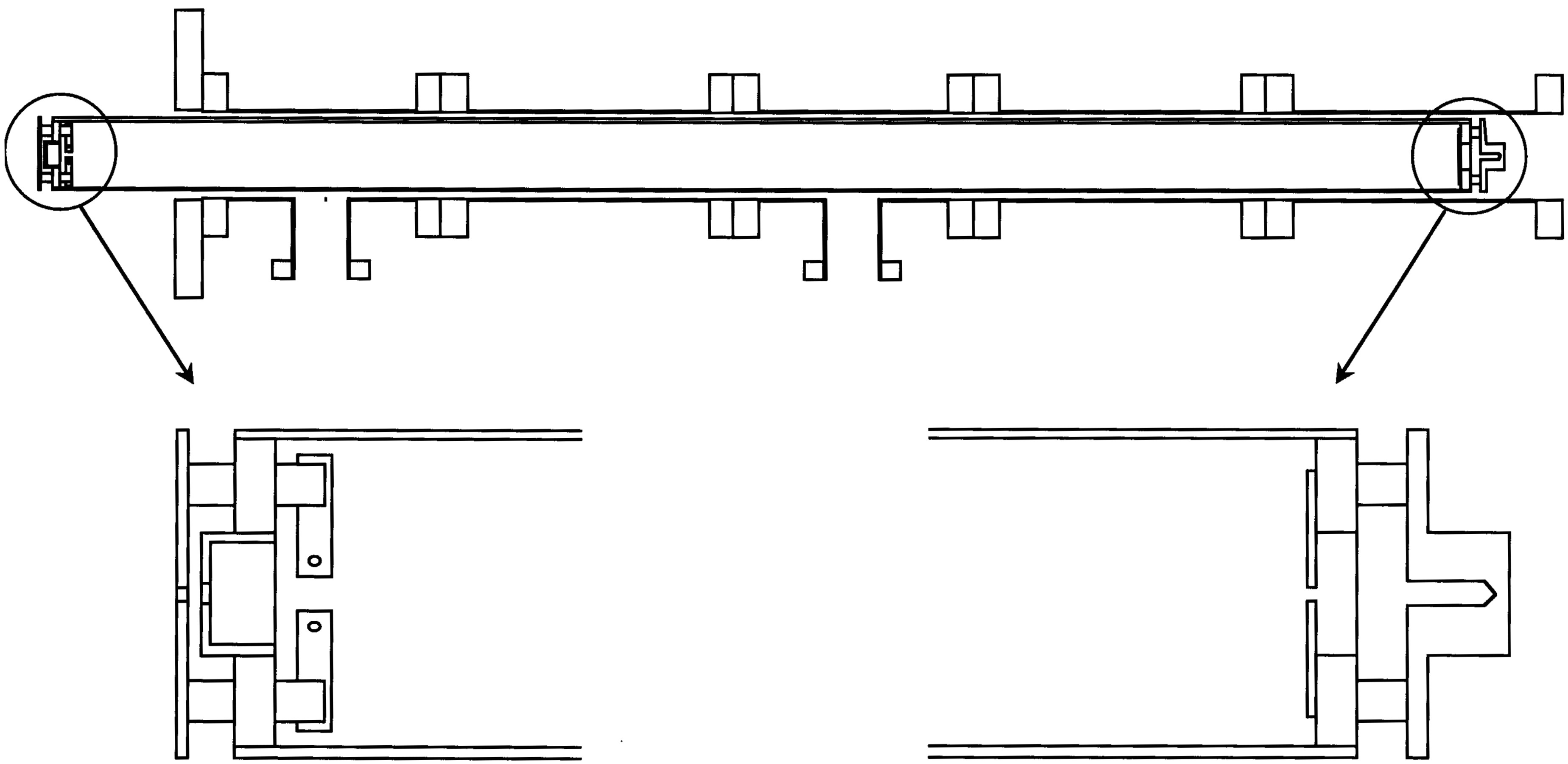

Inlet accelerator and gate electrodes

Exit aperture and collector cup

Vacuum Arc Thruster Test Chamber and Mass Spectrometer

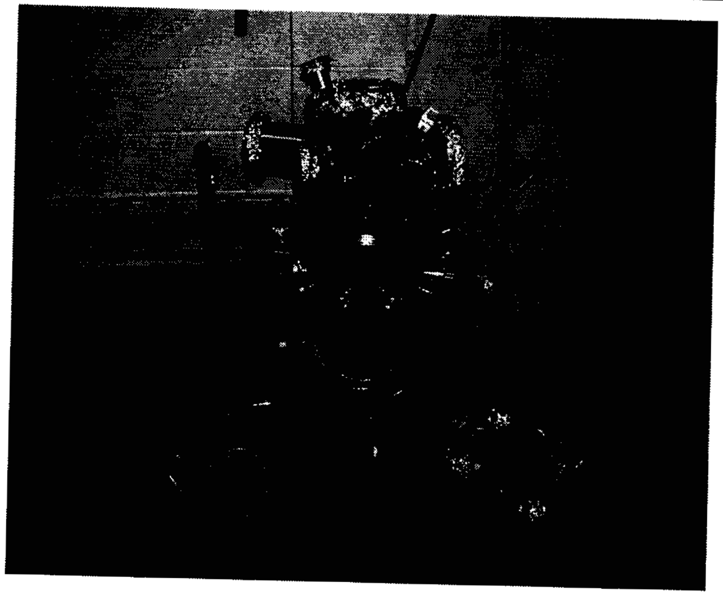

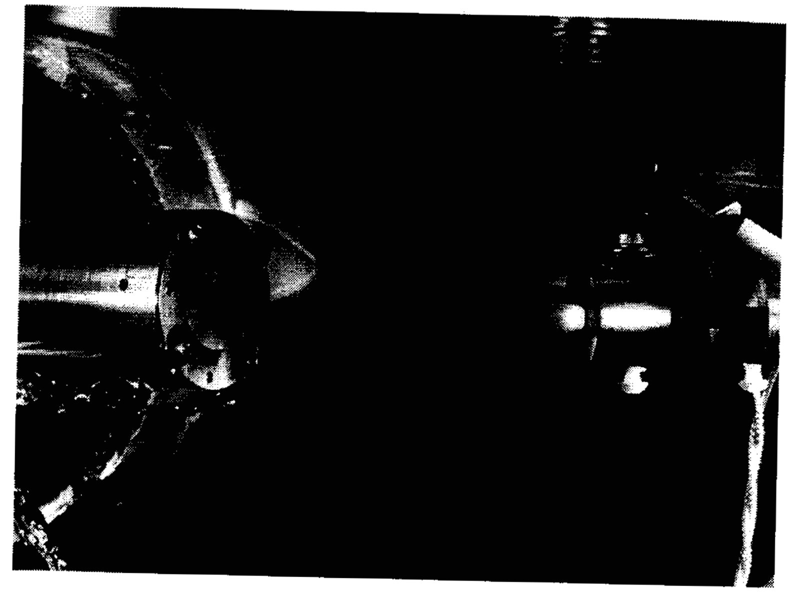

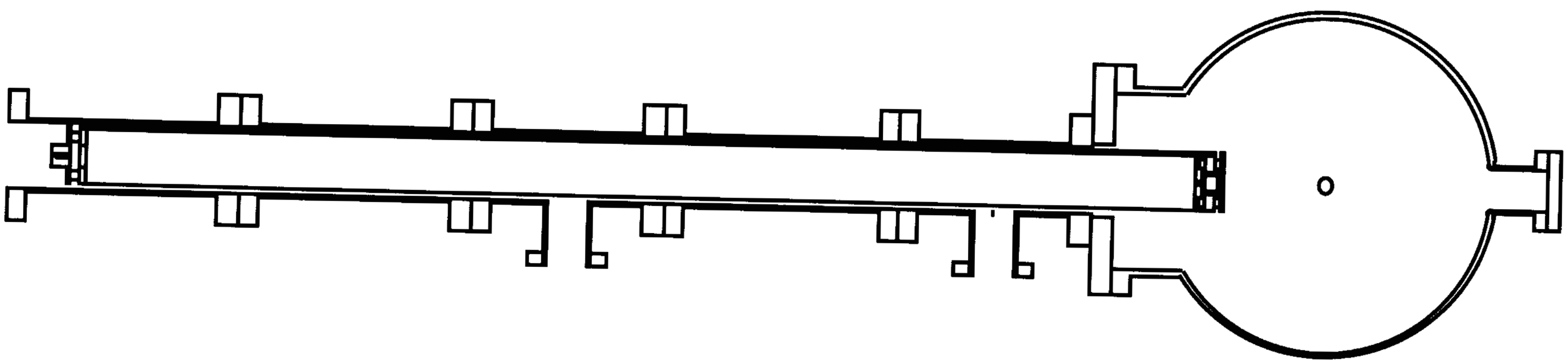

Angular Distribution of Charge State

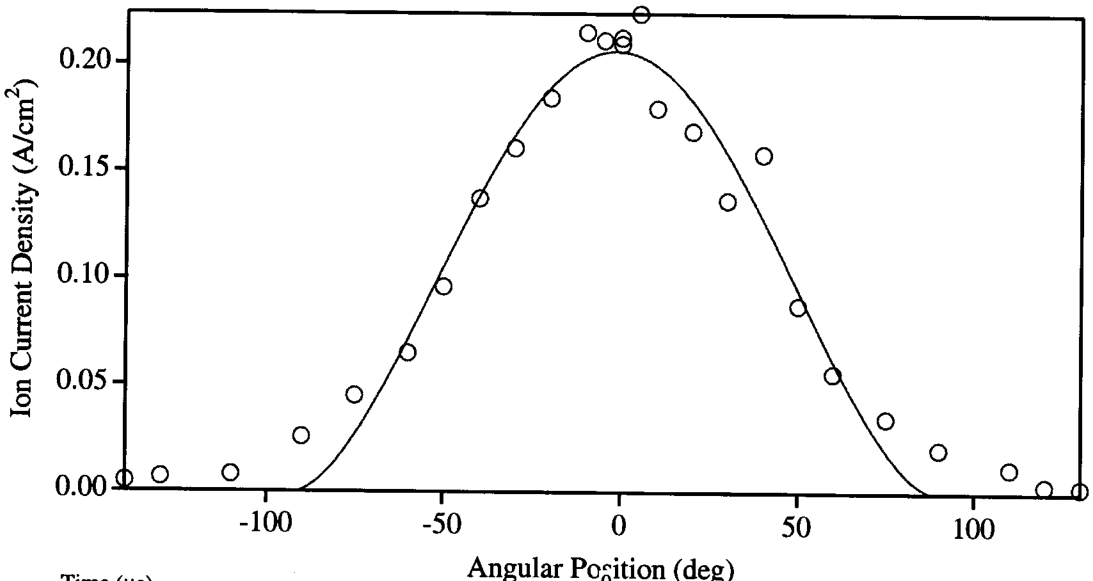

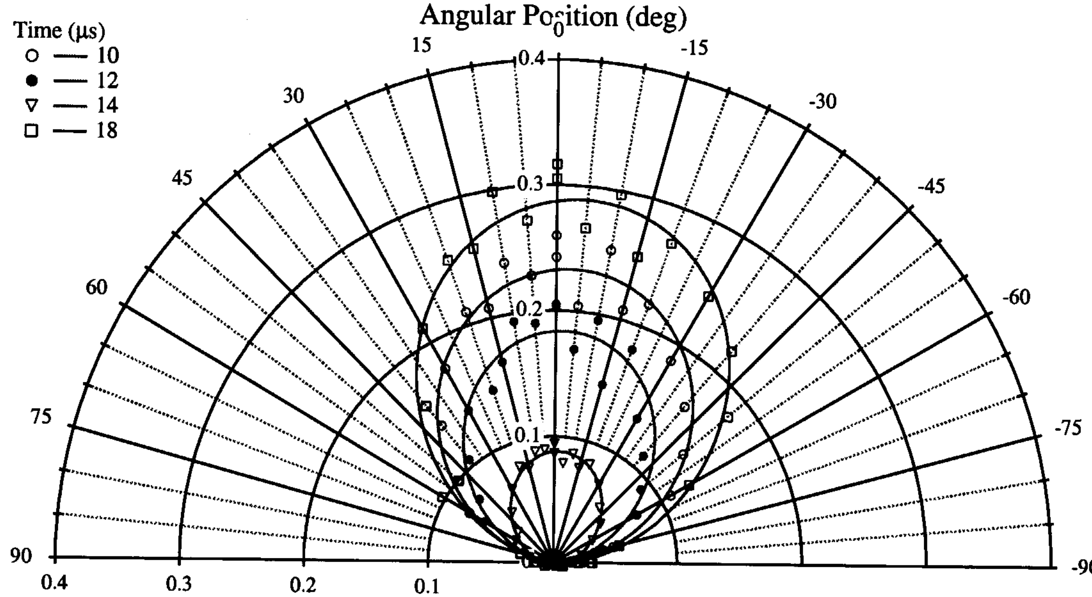

Material Properties Used to Estimate VAT and VAIT Performance Potential

Species	Mass M_i (AMU)	Ion Charge State Distribution f_1	f_2	f_3	f_4	f_5	f_6	$\langle Z^{-1} \rangle$	$\langle Z^{-1/2} \rangle$	Erosion Rate E_r (μg/C)	Ion Fraction F_i	Discharge Voltage V_d (V)	Ion Velocity u_i (m/s)
Li	6.941	1.000						1.00	1.00			23.5	23800
C	12	1.000						1.00	1.00	17	0.732	29.6	29700
Mg	24.305	0.307	0.701					0.66	0.80	31	0.528	18.8	30600
Al	26.981	0.224	0.590	0.191				0.58	0.75	28	0.577	23.6	29900
Si	28.086	0.450	0.504	0.043				0.72	0.83			27.5	25800
Ca	40.08	0.042	0.943	0.016				0.52	0.72			23.5	25900
Sc	44.96	0.150	0.749	0.101				0.56	0.74			19.1	
Ti	47.9	0.052	0.739	0.207				0.49	0.69	30	0.815	21.3	16700
V	50.94	0.038	0.664	0.280	0.019			0.47	0.68			22.5	19300
Cr	52	0.048	0.638	0.296	0.019			0.47	0.68	20	1.265	22.9	19400
Mn	54.94	0.327	0.658	0.020				0.66	0.80			22	10800
Fe	55.85	0.139	0.747	0.115				0.55	0.73	48	0.663	22.7	11800
Co	58.93	0.200	0.682	0.121				0.58	0.75	44	0.802	22.8	11800
Ni	58.71	0.167	0.727	0.102				0.56	0.74	47	0.736	20.5	10900
Cu	63.55	0.080	0.612	0.291	0.019			0.49	0.69	35	0.914	23.4	12800
Zn	65.38	0.667	0.333					0.83	0.90	320	0.176	15.5	10400
Ge	69.74	0.429	0.571					0.71	0.83			17.5	11000
Sr	87.62	0.010	0.990					0.50	0.71			18	
Y	88.91	0.022	0.544	0.434				0.44	0.66	45	0.898	18.1	14300
Zr	91.22	0.004	0.364	0.523	0.109			0.39	0.62	53	0.691	23.4	15700
Nb	92.91	0.003	0.160	0.510	0.293	0.033		0.33	0.57			27	15500
Mo	95.94	0.006	0.137	0.480	0.327	0.049		0.33	0.57	36	0.903	29.3	17400
Pd	106.4	0.121	0.713	0.144	0.021			0.53	0.72			21.3	15700
Ag	107.87	0.062	0.570	0.350	0.019			0.47	0.68	140	0.373	23.6	12500
Cd	112.41	0.523	0.485					0.77	0.87	620	0.142	16	6800
In	114.82	0.471	0.507					0.73	0.83			17.5	5500
Sn	118.69	0.313	0.693					0.66	0.80	295	0.273	17.5	7500
Ba	137.33	0.000	1.000					0.50	0.71			18.3	6700
La	138.91	0.005	0.685	0.311				0.45	0.67			17.2	7000
Ce	140.12	0.014	0.787	0.199				0.47	0.69			17.9	7000
Pr	140.91	0.014	0.613	0.373				0.44	0.66			20	8700
Nd	144.24		0.765	0.235				0.46	0.68			19.7	
Sm	150.4	0.010	0.779	0.211				0.47	0.68			14.6	7400
Gd	157.25	0.009	0.691	0.300				0.45	0.67	55	1.347	21.6	7400
Dy	162.5	0.009	0.574	0.417				0.43	0.66			19.8	7400
Ho	164.93	0.009	0.574	0.417				0.43	0.66			20	8300
Er	167.26	0.004	0.534	0.445	0.017			0.42	0.65			19	8200
Yb	173.04	0.014	0.867	0.118				0.49	0.70			14.4	
Hf	178.49	0.010	0.164	0.522	0.287	0.017		0.34	0.58			24.3	9200
Ta	180.95	0.007	0.225	0.389	0.328	0.051		0.34	0.58	56	1.143	28.7	11100
W	183.85	0.006	0.147	0.413	0.333	0.080	0.019	0.32	0.56	55	1.111	31.9	14300
Ir	192.22	0.019	0.278	0.519	0.165	0.019		0.38	0.61			24.5	
Pt	195.09	0.057	0.663	0.260	0.019			0.48	0.69			22.5	6800
Au	196.97	0.070	0.761	0.168				0.51	0.71			19.7	5800
Pb	207.2	0.225	0.780					0.62	0.78	510	0.257	15.5	5400
Bi	208.98	0.692	0.291					0.84	0.90			15.6	4200
Th	232.04	0.000	0.166	0.124	0.166			0.17	0.27			23.3	9900
U	231.04		0.075	0.547	0.377			0.31	0.56			23.5	11400

VATs Show Promise as Simple, Miniature Pulsed Thrusters

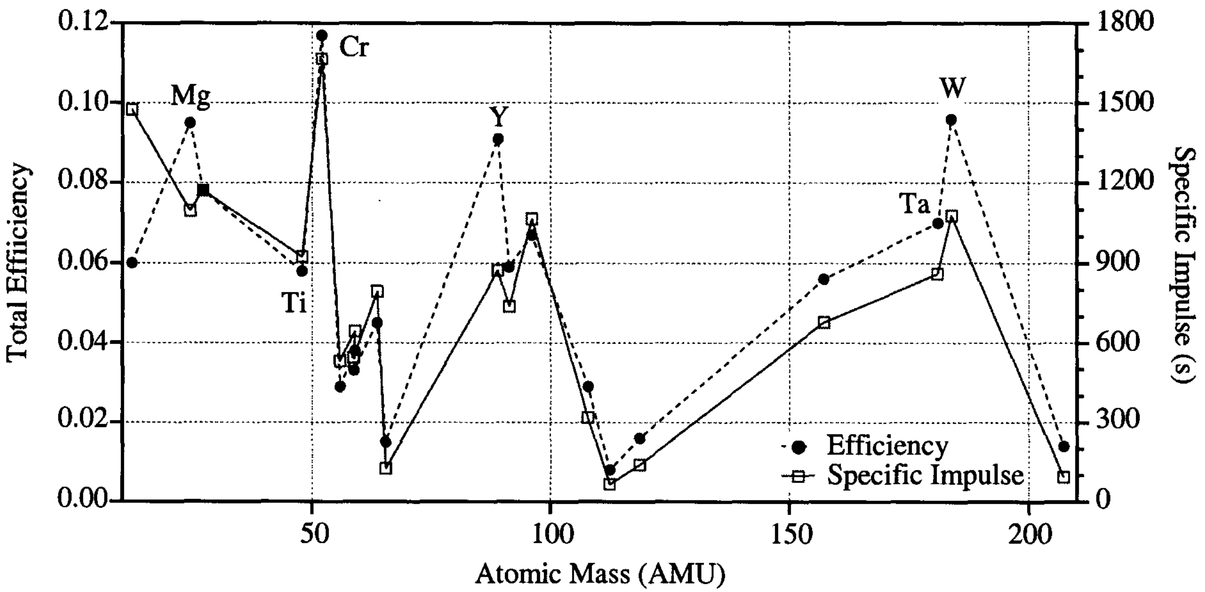

- Assumptions:
  - Jd = 10 A
  - fi = 0.1
  - Ct = 0.666
- Cr, Gd, Ta and W have unrealistically high values of ion mass fraction
  - fi < 0.1
  - Er > measured values

Species	Erosion Rate, E_r (μg/C)	Ion Current Fraction f_i	Ion Mass Fraction F_i	Vacuum Arc Thruster I_{sp} (s)	Vacuum Arc Thruster Total Efficiency η	Vacuum Arc Thruster Thrust-to-Power T/P (μN/W)	Vacuum Arc Ion Thruster I_{sp} (s)	Vacuum Arc Ion Thruster Propellant Efficiency η_u	Vacuum Arc Ion Thruster Total Efficiency η	Vacuum Arc Ion Thruster Thrust-to-Power T/P (μN/W)
Cr	20	0.100	1.265	1666	0.117	14.3	7143	0.81	0.585	16.4
	20	0.079	1.000	1316	0.073	11.3	5643	0.64	0.432	15.3
	25.3	0.100	1.000	1317	0.092	14.3	5647	0.64	0.462	16.4
Gd	55	0.100	1.347	677	0.056	16.9	4464	0.86	0.638	28.6
	55	0.074	1.000	501	0.031	12.5	3304	0.64	0.434	26.3
	74	0.100	1.000	503	0.042	16.9	3319	0.64	0.474	28.6
Ta	56	0.100	1.143	861	0.070	16.5	4050	0.73	0.493	24.4
	56	0.087	1.000	749	0.053	14.4	3523	0.64	0.410	23.3
	64	0.100	1.000	754	0.061	16.5	3544	0.64	0.432	24.4
W	55	0.100	1.111	1078	0.096	18.2	4029	0.71	0.464	23.1
	55	0.090	1.000	970	0.078	16.4	3626	0.64	0.402	22.2
	61	0.100	1.000	972	0.087	18.2	3632	0.64	0.418	23.1

VAITs Offer Much Higher Performance Capability

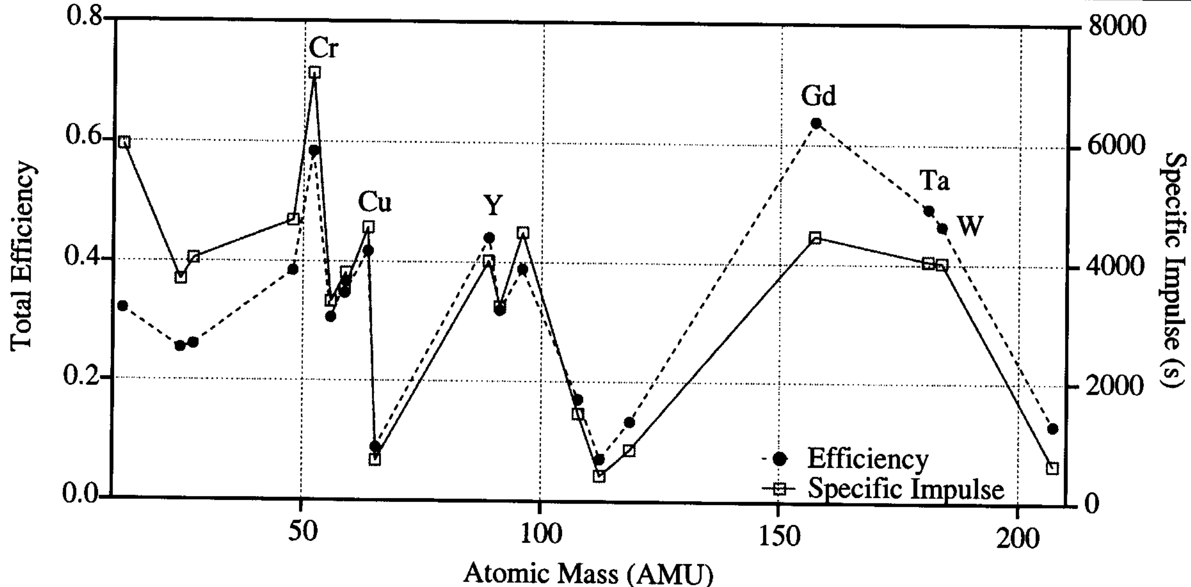

- Assumptions:
  - Jd = 10 A
  - fi = 0.1
  - Cj = 0.8
  - Transparency = 0.8
  - Vb = 1000 V
- Performance can be improved by increasing beam voltage

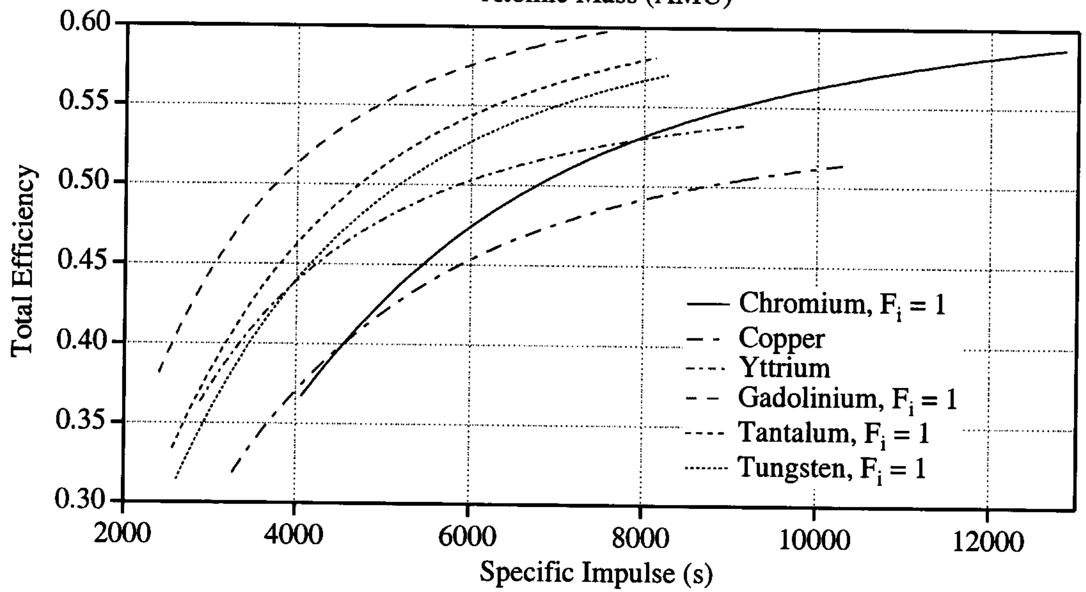

Conclusions

- A time-of-flight mass spectrometer adequately resolves the angular distribution of charge states in the plume of a vacuum arc thruster
- Charge state distributions measured for titanium agree well with measurements from Lawrence Berkeley National Laboratory
- The results indicate that the charge state does not vary dramatically with angle
- Models of vacuum arc thruster performance are not significantly affected by angular variation in charge state distribution